



# Ultrasonication for production of nanoliposomes with encapsulated soy protein concentrate hydrolysate: Process optimization, vesicle characteristics and *in vitro* digestion

Neda Pavlović<sup>a</sup>, Jelena Mijalković<sup>b</sup>, Verica Đorđević<sup>c</sup>, Danijela Pecarski<sup>d</sup>, Branko Bugarski<sup>c</sup>, Zorica Knežević-Jugović<sup>b,\*</sup>

<sup>a</sup> Innovation Center of the Faculty of Technology and Metallurgy, Karnegijeva 4, 11000 Belgrade, Serbia

<sup>b</sup> University of Belgrade, Faculty of Technology and Metallurgy, Department of Biochemical Engineering and Biotechnology, Karnegijeva 4, 11000 Belgrade, Serbia

<sup>c</sup> University of Belgrade, Faculty of Technology and Metallurgy, Department of Chemical Engineering, Karnegijeva 4, 11000 Belgrade, Serbia

<sup>d</sup> Academy of Applied Studies Belgrade, The College of Health Sciences, Cara Dušana 254, Belgrade, Serbia

## ARTICLE INFO

### Keywords:

Soy protein concentrate  
Enzymatic hydrolysis  
Hydrolysate encapsulation  
Liposome-peptides carriers  
Antioxidant activity  
Structural characterization  
*In vitro* digestion

## ABSTRACT

This study presents the state-of-art research about the assembly of soy proteins in nanocarriers, liposomes, and its design includes different physicochemical strategies and approaches: two-step enzymatic hydrolysis of soy concentrate, hydrolysate encapsulation by using phospholipids and cholesterol, and application of ultrasonication. Achieved results revealed that ultrasonication, together with cholesterol addition into phospholipid layers, improved the stability of nanoliposomes, and a maximum *EE* value of 60.5 % was obtained. Average size of peptide-loaded nanoliposomes was found to be from 191.1 to 286.7 nm, with a  $\zeta$  potential of  $-25.5$  to  $-34.6$  mV, and a polydispersity index of 0.250–0.390. Ultrasound-assisted encapsulation process did not lead to a decrease in the antioxidant activity of the trapped peptides. FTIR has indicated an effective hydrophobic interaction between phosphatidylcholine and hydrolysate peptides. TEM and SEM have confirmed the spherical nanocarrier structure and unilamellarity. Prolonged gastrointestinal release and stability of peptides have been enabled by liposome nanocarriers.

## 1. Introduction

Foods are being utilized to prevent from chronic illnesses such as hypertension, coronary artery disease, osteoporosis, and others, in addition to delivering nutrients and meeting metabolic demands. Functional foods have played a significant influence in this respect, due to fortification of food matrix with ingredients, micronutrients, or naturally occurring compounds, having favorable effects on health and disease prevention (Xu et al., 2021). Furthermore, protein hydrolysates are increasingly being used in the variety of functional food formulations, especially plant protein hydrolysates, abundant in bioactive peptides. When compared to intact proteins, the protein hydrolysates have a lower molecular weight and a relative lack of high-order structure, as well as a higher number of functionally ionizable and exposed hydrophobic groups. These characteristics indicate that hydrolysates may differ from intact proteins in terms of surface interactions, water solubility, digestibility, host-receptor interactions, and biological activity as

toxicity, allergenicity, antioxidant, and other activities (Jovanović et al., 2019; Tkaczewska, 2020; Krobthong et al., 2021). Endopeptidases, such as commercially available Alcalase and Neutrase, are extensively utilized in the production of bioactive peptides. These endopeptidases liberate peptides by cleaving mainly hydrophobic amino acid peptide bonds in the protein chain, resulting in peptides with hydrophobic amino acid residues at *N*- and/or *C*-terminus (Chang et al., 2021). According to the literature, these hydrophobic amino acid residues are linked to the peptides' distinctive bitter taste, which hinders consumer acceptability and limits their use in the food industry. Debittering by enzymatic hydrolysis is a procedure that uses broadly applied exopeptidases, or a combination of endopeptidases and exopeptidases, to remove the hydrophobic amino acids associated with bitterness at *N*- or *C*-terminus of peptides (Zhao, Schieber, & Gänzle, 2016).

It appeared that, considering the protein content and global production data, the main plant protein sources are cereals and legumes (Görgüç et al., 2020). Among legumes, soybean has valuable amounts of

\* Corresponding author at: University of Belgrade, Faculty of Technology and Metallurgy, Karnegijeva 4, 11000 Belgrade, Serbia.

E-mail address: [zknez@tmf.bg.ac.rs](mailto:zknez@tmf.bg.ac.rs) (Z. Knežević-Jugović).

protein, making it to be the most used protein source. Namely, soybean products contain high level of crude proteins, rich in essential amino acids: 45 % in the form of flour, 70 % in the form of concentrate and even 90 % in the form of isolates. Thus, the production of soy protein hydrolysates is very perspective, popular and profitable. Produced bioactive peptides obtained from soy protein forms have dual role, to improve health related functions and to enhance technological properties of foods (Chatterjee, Gleddie, & Xiao, 2018; Jovanović et al., 2019; Görgüç et al., 2020). Precisely, soy peptides have contributed to the reduction and prevention of *in vivo* chronic diseases such as diabetes, hypertension, and obesity, and possess the great ability as hypolipidemic, antioxidant, antimicrobial, antihypertensive, anticancer, anti-inflammatory, immunostimulatory and neuromodulatory agents (Chatterjee, Gleddie, & Xiao, 2018; Li et al., 2022). However, the structural and biological instability of peptides during commercial processing and under human physiological conditions is a major barrier to its incorporation into functional food ingredients. As a result, before reaching the target cells or organs, bioactive peptides may lose some or all of their activities. Thus, recent studies, focused on the soy peptide quantity released by *in vivo* or *in vitro* digestion methods, are warranted for a better understanding of peptide absorption and metabolism, as well as to select a delivery mechanism that is well-suited to human physiological conditions (Daroit & Brandelli, 2021).

The controlled release of the bioactive agents at the target site is made easier with the encapsulation approach. Because of the heterogeneous chemical bonds inherent in protein hydrolysates, bioactive peptide encapsulation is more challenging than encapsulation of other bioactive compounds such as vitamins, aromas, and polyphenols (McClements, 2014). This strategy has the following advantages: well-maintained organoleptic qualities, masking the bitter taste caused by hydrophobic amino acid residues, enhanced bioavailability and stability, and protection from intestinal enzymes (Mohan et al., 2015). In the literature, there are several encapsulation strategies for bioactive hydrolysates or peptides, among which liposomes carriers stand out due to the compatibility with a wide range of bioactive compounds (McClements, 2014; Jash, Ubeyitogullari, & Rizvi, 2021; Ramezanzade et al., 2021). However, despite several advantages of liposomes, studies on their applications for encapsulation of protein hydrolysates or bioactive peptides are rather recent (Corrêa, et al., 2019; Jash, Ubeyitogullari, & Rizvi, 2021; Sepúlveda, et al., 2021).

Liposomes are spherical vesicles with a core aqueous phase enclosed by one or more phospholipid bilayers. Because of the unusual amphiphilic nature, liposomes may encapsulate a wide spectrum of bioactive compounds for delivery, including both hydrophobic and hydrophilic molecules. Liposomes, which are remarkably similar to cell membranes, are ideal for encapsulating bioactive peptides, that must be administered orally (Jash, Ubeyitogullari, & Rizvi, 2021). Besides, liposomes have an advantage over other carriers since the components used for its production could be of low cost, which increases its commercial feasibility. The results of recent studies imply the efficacy of liposomes in protection, control of release and maintaining the bioactivities of hydrolysates or peptides from several sources like orange seed protein hydrolysate (Mazloomi, et al., 2020), casein protein hydrolysate (Sarabandi et al., 2019a), flaxseed protein hydrolysate (Sarabandi et al., 2019b), fish protein hydrolysates (Li, Paulson, & Gill, 2015; Sepúlveda, et al., 2021), whey protein hydrolysate (Corrêa, et al., 2019), sunflower protein hydrolysate (Luo, & He, 2018), *Spirulina plantensis* protein hydrolysate (Mohammadi, et al., 2021), and others. Also, the use of liposomes improves organoleptic qualities, increases bioavailability and stability, and allows regulated release of bioactive peptides, with the magnitude of these improvements depending on the chemical nature of the encapsulated hydrolysate, and the liposome preparation and size reduction process utilized (Corrêa et al., 2019; Luo & He, 2018; Sarabandi et al., 2019b; Sarabandi, Mahoonak, Hamishehkar, Ghorbani, & Jafari, 2019a; Sepúlveda, Alemán, Zapata, Montero, & Gómez-Guillén, 2021).

However, the liposomes' drawbacks as encapsulation carriers stem

from their low stability as a result of lipid oxidation and hydrolysis, colloidal particle breakage and fusion, and the loss of the hydrophilic core. These drawbacks are successfully mitigated by the use of stabilizers, antioxidants, and post-processing techniques such as freeze-drying (Nkanga, et al., 2019). Soy protein hydrolysate can act as a stabilizer; in fact, a hydrolysate derived from soy isolate improves liposomal stability by inhibiting primary and secondary lipid oxidation products (Chen et al. 2020). In two recent studies (Chen et al. 2020, 2021) the mechanism of the interactions between the hydrolysate and phospholipid was thoroughly investigated, as well and the effects of the interactions on liposome oxidation and stability. Inspired by that and from the viewpoint of technological aspects, the main aim of this study is to create a stable liposome formulation for controlled delivery of soy protein hydrolysate. Keeping in mind the economic feasibility of such formulations in industry, the hydrolysate will be obtained by enzymatic hydrolysis of soy protein concentrate, thus avoiding the purification step necessary when producing an isolate from the concentrate. Besides, the specific goal of this research is to contribute to the application of ultrasound-assisted loading approach during the design of new multi- and unilamellar nanoliposomes with encapsulated antioxidant soy hydrolysate. The optimization of the liposome formation protocol will be carried out by varying the concentration of peptides and phospholipid, and adding cholesterol. Particularly, the potential of nanoliposomes' utilization as carriers of antioxidant soy protein hydrolysate will be examined in the simulated gastrointestinal tract.

## 2. Materials and methods

### 2.1. Materials

Soy protein concentrate (TRADCON F200; granulation: min 90 % <0.075 mm; protein content 68 % on dry basis) was kindly procured from SOJAPROTEIN d.o.o. Bečej, Serbia. The commercial available proteolytic enzymes Neutrase® (protease from *Bacillus amyloliquefaciens*; ≥ 0.8 U/g) and Flavourzyme® (protease from *Aspergillus oryzae*, ≥ 500 U/g) were purchased from Sigma Aldrich (St. Louis, MO, USA). The nanoliposomes have been fabricated with Phospholipon®90G, a commercial lipid mixture containing more than 94.0 % of phosphatidylcholine, 4.0 % of lysophosphatidylcholine and 0.3 % of tocopherol (Phospholipid GmbH, Köln, Germany). Cholesterol, Tween-80 and chloroform p.a. were provided by Sigma Aldrich (St. Louis, USA), Acros Organics (Geel, Belgium), and Lachner (Neratovice, Czech), respectively. The antioxidant activity of hydrolysate-loaded nanoliposomes has been tested using the following chemicals: 2,2'-azino-bis(3-ethylbenzothiazoline-6-sulfonic acid)-diammonium salt (ABTS; Alfa Aesar, Massachusetts, USA), iron(II) chloride, 3-(2-pyridyl)-5,6-diphenyl-1,2,4-triazine-4',4''-disulfonic acid (Ferrozine), 6-hydroxy-2,5,7,8-tetramethylchromane-2-carboxylic acid (Trolox) and linoleic acid (Sigma Aldrich, St. Louis, MO, USA), ethylenediaminetetraacetic acid disodium salt dihydrate (Tokyo Chemical Industry UK Ltd., Oxvord, UK) and *L*-ascorbic acid (Fisher Scientific, Waltham, MA, USA). *In vitro* gastrointestinal digestion of nanoliposomes was assessed using the pepsin (Sigma Aldrich, St. Louis, USA), bile salts (Biolife Italiana S.r.l, Milan, Italy), and pancreatin (MP Biomedicals, Illkirch-Graffenstaden, France). All other chemicals used were of analytical grade.

### 2.2. Enzymatic hydrolysis of soy protein concentrate

The two-step hydrolysis of soy protein concentrate was performed with Neutrase and Flavourzyme, since this process yielded the hydrolysate with the highest antioxidant activities as described in a previous work (Knežević-Jugović et al., 2018). Namely, among the six enzymes tested (papain, Alcalase, Neutrase, Everlase, Umamizyme and Flavourzyme) and their combination in one-step and two-step processes, the combination of Neutrase and Flavourzyme was shown to be the most desirable for producing high quality soy protein hydrolysate because of

the low bitterness score combined with a high solubility, moderate rheological properties and the highest free radical scavenging activity determined by three methods (Culetu et al., 2018; Culetu et al., 2019). The enzymatic hydrolysis of dispersed 8 wt% soy protein concentrate (SPC) was performed in a mechanically stirred batch reactor with total volume of 400 mL. The stirring was acquired by a three-bladed propeller at 200 rpm while the temperature was automatically regulated with a thermocouple as described (Jovanović et al., 2019). After completion of hydration and pre-incubation of the soy concentrate suspension, at the optimum pH and temperature (pH 7, 45 °C) for 20 min, the hydrolysis reaction was initiated by the addition of endoprotease Neutrase at a constant *E/S* ratio of 4 wt%. At the achieved degree of hydrolysis approx.  $6.20 \pm 1.50$  %, upon 75 min of reaction, the pH and temperature of the reaction mixture were adjusted to the optimal ones for the second enzyme endo- and exoprotease Flavourzyme, 7 and 50 °C, respectively. The Flavourzyme has been added at the equal *E/S* ratio. The degree of hydrolysis was monitored by quantifying the content of hydrolyzed peptide bonds over 285 min using the ninhydrin method, as described in the protocol of Starcher (2001). The hydrolysis reaction was stopped by inactivation of the enzyme in a boiling water bath (10 min) after 285 min of hydrolysis, i.e. at the moment when the equilibrium state was observed by measuring the degree of hydrolysis ( $DH \approx 24.20 \pm 2.85$  % for at least three consecutive experimental points). Afterwards, the mixture was cooled to room temperature and centrifuged at  $10,000 \times g$  for 10 min and 4 °C (Fresco™ 17 Microcentrifuge, Thermo Fisher Scientific, Waltham, MA, USA). The precipitate was disposed away, and the supernatant, i.e. soy protein hydrolysate (SPH) – mixture of soy peptides has been spray dried (Mini Buchi B-290 spray-dryer, BÜCHI Labortechnik AG, Switzerland), weighed, analyzed for crude protein content according to the standardized Kjeldahl method (ISO 5983-2:2005), and used for further encapsulation protocol. The average molecular weights (MW) of the peptides present in the hydrolysates were determined by membrane separation techniques. The hydrolysate was sequentially fractionated through ultrafiltration, using four membranes with different molecular weight cut off (MWCO) of 1, 3, 10 and 30 kDa (Mulpore, USA) in an ultrafiltration cell (Model 8050 1 unit, Amicon, USA). Five fractions were separated: fraction I with MW higher than 30 kDa, fraction II with MW between 10 and 30 kDa, fraction III with MW between 1 and 10 kDa and fraction IV with MW lower than 1 kDa. The peptide concentration was determined by the modified Lowry method (Hartree, 1972). The amino acids profile in the hydrolysate was composition determined by high performance anion-exchange chromatographic technique coupled with integrated pulsed amperometric detection (HPAEC-IPAD) followed the standardized protocol. The content of free amino acids in the samples after enzymatic hydrolysis, as well as in the peptide fraction after membrane separation was determined by used ninhydrin spectrophotometric technique (Starcher, 2001).

### 2.3. Encapsulation of soy protein hydrolysate into nanoliposomes

Liposome nanoparticles were generated utilizing a thin film hydration method according to Pavlović et al. (2020), with slight changes. Two approaches were used as techniques to stabilize liposome carriers in physiological media: 1) without the inclusion of cholesterol; and 2) with the addition of cholesterol. The preparation technique will be briefly described. Initially, 0.3 g of phospholipon, 0.014 g of Tween-80 and 0.05 g of cholesterol (only in the formulation with cholesterol) were completely dissolved in 15 mL of chloroform for 15 min. The resultant solution was transferred to a round-bottom flask, and the whole solvent evaporation process as well as thin-film creation on the inner walls were carried out using a rotary evaporator (Rotavapor® R-210, BÜCHI Labortechnik AG, Flävil, Switzerland) at 70 rpm, 50 °C, and 323 mbar. After evaporating of chloroform by rotary evaporator, the flasks with thin-film were placed on a vacuum system for 1 h at 40 °C to remove residual chloroform and then the flasks were left in the chapel overnight

to dry completely the lipid film. In five cycles, 15 mL of preheated soy protein hydrolysate solution, containing 15, 30, 45, and 60 mg of peptides, was used to hydrate the dried thin-film through a process involving 2 min vortexing at ambient temperature and 2 min of stirring at 60 °C. Finally, the resultant suspension of multilamellar liposome carriers was ultrasonicated by using an ultrasound probe TT13 (HD 2200, Sonopuls Ultrasonic Homogenizers, Bandelin, Germany) at a nominal frequency of  $20 \text{ kHz} \pm 500 \text{ Hz}$  and 30 % of amplitude. The overall liposome ultrasonication was consisted of two phase mode: 1) sonicated phase with duration of 20 sec at pulsed cycle mode set to two and 2) non-sonicated (standing) phase with duration of 1 min. Both of these phases were performed alternately, three times each. During the ultrasonication procedure, the temperature of liposome suspension has been kept constant at 5–6 °C with an ice bath, so that the temperature effect of the sonification could be neglected.

The phospholipid mass was then optimized following selection of the most suitable mass of hydrolysate peptides. The preparation technique was carried out in an identical manner, with the exception that 0.15, 0.3, 0.45, 0.75, and 1.50 g of phospholipids were dissolved in 15 mL of chloroform. Furthermore, the same process was followed to make empty nanoliposomes with and without cholesterol, with the exception that instead of the peptide sample, 15 mL of Tris-HCl buffer (0.01 M, pH 7) was utilized. The nanoliposomes were fabricated in triplicate and stored in the refrigerator until testing time.

### 2.4. Characterization of soy hydrolysate-loaded nanoliposome carriers

#### 2.4.1. Encapsulation efficiency

The mass of encapsulated soy hydrolysate peptides was determined indirectly by measuring the concentration of non-encapsulated peptides in the fabricated nanoliposome suspension, which was centrifuged at 40,000 rpm for 30 min at 4 °C (Optima™ L-100 XP Ultracentrifuge, Beckman Coulter, Brea, California, USA). The supernatant was decanted and used thereafter for quantitative protein content analysis. A quantitative determination of total proteins content introduced into the system at the beginning of the encapsulation procedure and non-encapsulated proteins remaining in the supernatant was performed by the modified Lowry method (Hartree, 1972). The encapsulation efficiency, *EE*, was calculated by the following equation (Eq. (1)):

$$EE(\%) = \frac{m_{\text{enc}}}{m_t} \cdot 100 = \frac{m_t - m_{\text{sn}}}{m_t} \cdot 100 \quad (1)$$

where  $m_{\text{enc}}$  is the mass of encapsulated peptides,  $m_t$  is the total mass of the soy peptides used for the preparation of the liposomes, and  $m_{\text{sn}}$  is the soy peptide mass in the supernatant.

#### 2.4.2. Determination of size, polydispersity, $\zeta$ potential and stability

Using pure deionized water, soy hydrolysate-loaded liposome (SHL) samples were first diluted 1000-fold. The mean particle size ( $z$ -average, nm) and polydispersity index (PdI) of fresh and incubated liposome suspension were measured by a dynamic light scattering system Zetasizer Nano series (NanoZS, Malvern Instruments Ltd., UK) at 90° angle and 25 °C in a cell specified to the system with a 1 cm width. The average of at least 8 consecutive measurements was used for particle size analysis, with each measurement being the average of 14 measurements.

The surface electrical charge of nanoliposomes,  $\zeta$  potential (mV), was evaluated using the same setup, by an electrophoretic mobility technique and monitoring the particle's motion in the electric field. For one  $\zeta$  potential measurement, ten consecutive measurements were taken. The  $\zeta$  potential measurements were taken again after 7, 14, 21, and 60 incubation days at 4 °C to check liposome stability. Every sample was examined three times, with the average values of these measures being displayed.

### 2.4.3. Structural and morphological characteristics of soy hydrolysate-loaded nanoliposomes

Before doing ATR-IR spectroscopy in order to evaluate chemical structure, the empty and peptide-loaded liposomes were freeze-dried to create a solid form. A little amount of saccharose (2 wt%) was added to the liposome solution as a cryoprotectant during the lyophilization process. The spectra of pure soy protein hydrolysate, empty liposome and soy hydrolysate-loaded liposome powder samples, as well as the thin phospholipid film after complete evaporation and drying processes, were acquired in transmission mode using a Nicolet™ iSTM10 FT-IR spectrometer (Thermo Fisher Scientific, Madison, USA) with Smart iTR™ attenuated total reflectance (ATR) sampling accessories. ATR-FTIR spectra (20 accumulated scans at 4 cm<sup>-1</sup> resolution) were collected over the frequency range of 500 to 4000 cm<sup>-1</sup>. The spectra of each sample were performed in triplicate and the results were reported as the averages of these replicates (relative standard deviation < 5 %).

The carriers morphology study of soy hydrolysate-loaded nanoliposome was carried out with TEM analysis. The 8 µL droplet from empty liposome and hydrolysate-loaded liposome were deposited on the carbon coated grids (Agar Scientific Ltd., Stansted, Essex, UK), fixed and dried, contrasted with uranyl acetate and examined by a transmission electron microscope (Philips CM12, FEI, Oregon, USA) at 80 kV equipped with the SIS MegaView III camera (Olympus Soft Imaging Solutions, Münster, Germany). All these measurements and analyses were performed using TEM software (Olympus Soft Imaging Solutions, Münster, Germany). Besides, the morphology of nanoliposomes was analyzed by scanning electron microscopy (Tescan MIRA 3 XMU, Brno, Czech Republic) at an accelerating voltage of 5 kV. Prior to the SEM analysis, the powder nanoliposomes were coated with gold in a sputter coater (Polaron SC502, Thermo VG Microtech, West Sussex, UK) under an Ar atmosphere (50 Pa at 50 mA for 50 s) in order to avoid electrostatic charge.

## 2.5. Evaluation of antioxidant activity of the soy hydrolysate-loaded nanoliposomes

### 2.5.1. ABTS<sup>•+</sup> radical scavenging activity

The ABTS<sup>•+</sup> radical scavenging activity of nanoliposomes was determined using the procedure described by Pavlović et al. (2020). The ABTS<sup>•+</sup> solution was prepared by mixing the 7 mM ABTS with 140 mM potassium persulfate (so that a final concentration of 2.45 mM was achieved). Before use, the final ABTS<sup>•+</sup> solution was stored in the dark at room temperature for 12–16 h. The radical cation solution was diluted with 5 mM PBS buffer (pH 7.4) to an absorbance rate of 0.70 ± 0.02 at 734 nm before testing. An aliquot (10 µL) of each hydrolysate-loaded liposomes was mixed with 1 mL of radical cation solution. The antioxidant activity was quantified measuring the absorbance rate at 734 nm (UV-vis spectrophotometer, Ultrospec 3300 Pro, Amersham Bioscience, UK) after 5 min incubation in the dark. The control sample was made in the same way, except instead of a sample, it contained PBS buffer. The degree of scavenging activity expressed in a percentage was calculated as the ratio of the reacted amount and the total amount of radical cation:

$$ABTS(\%) = \frac{ABTS_{\text{reacted}}}{ABTS_{\text{total}}} \cdot 100 = \frac{A_{\text{control}} - A_{\text{sample}}}{A_{\text{control}}} \cdot 100 \quad (2)$$

where  $A_{\text{control}}$  and  $A_{\text{sample}}$  represent the reading absorbances of control and sample (Eq. (5)), respectively.

A standard curve was plotted by reacting 10 µL of Trolox (0, 20, 40, 70, 200, 400, 600, 800 µM) with 1 mL of diluted ABTS<sup>•+</sup> solution. The ABTS radical inhibition activity of each hydrolysate-loaded liposome was presented as Trolox equivalent antioxidant activity (TEAA, µmol).

### 2.5.2. Metal-ion chelating activity

The metal-ion chelating activity of nanoliposomes was measured using an approach published by Pavlović et al. (2020). Briefly, the

samples were made by mixing 0.2 mL of each hydrolysate-loaded liposome with 0.8 mL of deionized water. After that, 0.1 mL of a 2 mM reagent solution of FeCl<sub>2</sub> was added, intensively was vortexed, and was incubated for 3 min at 20 °C. Following the incubation period, 0.2 mL of 5 mM ferrozine solution was added. The mixture was incubated at 20 °C for 10 min after rigorous mixing. The control sample was made in the same way, except instead of a sample, it contained deionized water. The Fe<sup>2+</sup> chelating activity was quantified using UV-vis spectrophotometer (UV/Vis Ultrospec 3300 Pro, Amersham Bioscience, UK) by measuring the change in the absorbance of the Fe<sup>2+</sup>-ferrozine complex at 562 nm. The degree of metal-ion chelating activity (MICA, %) was calculated as the amount of the reacted over the total amount of Fe<sup>2+</sup> ions:

$$MICA(\%) = \frac{Fe^{2+}_{\text{reacted}}}{Fe^{2+}_{\text{total}}} \cdot 100 = \frac{A_{\text{control}} - A_{\text{sample}}}{A_{\text{control}}} \cdot 100 \quad (3)$$

where  $A_{\text{control}}$  and  $A_{\text{sample}}$  represent the reading absorbances of control and sample (Eq. (5)), respectively.

A standard curve was plotted by reacting 0.2 mL of EDTA (0, 20, 50, 100, 150, 200, 250, 300 µM) with reactants of the above described protocol. The capacity of each hydrolysate-loaded liposome to chelate Fe<sup>2+</sup> ions was presented as EDTA equivalent antioxidant activity (EEAA, µmol).

### 2.5.3. Lipid peroxidation inhibitory activity

The ammonia-thiocyanate method was used to measure lipid peroxidation inhibition activity, which was modified slightly from a previous protocol (Memarpoor-Yazdi, Asoodeh & Chamani, 2012). Shortly, the soy protein hydrolysate, empty liposome and soy hydrolysate-loaded liposome samples were diluted with 50 mM phosphate buffer (pH 7) to reach a peptide concentration of approximately 200 ppm. The reaction samples were prepared in an erlenmeyer flask with a reaction volume of 10 mL in the absence of light. Aliquots of 10 mL of absolute ethanol and 0.13 mL of linoleic acid were consecutively added, the mixture was homogenized and the reaction flasks were filled with deionized water up to 25 mL. Concurrently, the positive and negative controls were prepared by using ascorbic acid and phosphate buffer, respectively, instead of peptide samples. For facilitating the oxidation process of linoleic acid, the reaction flasks were incubated in the dark at 50 °C for 7 days.

During the incubation period, 0.1 mL of the reaction mixture was taken at every 24 h, and the lipid oxidation rate was measured by the ammonia-thiocyanate method. This method involved mixing the pipetted aliquot with 75 wt% ethanol (4.7 mL), 30 wt% ammonium thiocyanate (0.1 mL) and 20 mM FeCl<sub>3</sub> (0.1 mL; dissolved in 3.5 wt% HCl). After vortexing and incubation of 3 min at 20 °C, the changes in the absorbance at 500 nm were measured. The degree of lipid peroxidation inhibition was calculated according to the following equation:

$$LPI(\%) = \frac{A_c - A_s}{A_c} \cdot 100 \quad (4)$$

where  $A_s$  is the absorbance of the sample (Eq. (5)), while  $A_c$  is the absorbance of the negative control.

In the case of hydrolysate-loaded liposome formulation, the “sample”, for all three methods, represents the absorbance of the encapsulated peptides, which is calculated as:

$$A_{\text{sample}} = A_t - A_{\text{sn}} \quad (5)$$

where  $A_t$  is the absorbance of total soy peptides in the liposome formulation, and  $A_{\text{sn}}$  is the absorbance of non-encapsulated soy peptides in the supernatant.

## 2.6. Controlled soy hydrolysate release in gastrointestinal tract simulation

*In vitro* gastrointestinal (GI) digestion catalyzed by pepsin and pancreatin was performed in batch system by the described method of



Gomaa et al. (2017) with minor modifications. The controlled release was monitored in two types of solutions that simulate the GI conditions: gastric and pancreatic juice. Gastric juice was prepared by dissolving 0.2 g NaCl in 0.7 mL of 5 M HCl solution. Then, pH was adjusted to 1.4, the pepsin was added at a concentration of 3.2 mg/mL, and was filled up to 100 mL with distilled water. Gastric juice solution was incubated at 37 °C and thus used for digestion. Concurrently, 6.8 g of dipotassium hydrogen phosphate was dissolved in a little amount of deionized water to make pancreatic juice. After that, pH was raised to 7.4 by using 2 M solution of sodium hydroxide, bile salts at a concentration of 0.2 mg/mL were added, and the flask was filled up to 100 mL with distilled water. Pancreatin juice solution was incubated at 37 °C, and then the solid pancreatin (20 mg/mL) was added.

The digestion in the gastric and pancreatic juice was performed by mixing the soy protein hydrolysate or soy hydrolysate-loaded liposome and the corresponding juice at the volume ratio 1:3. The digestions catalyzed by pepsin and pancreatin juices were performed at 37 °C in a thermo-shaker (Digital Heating Shaking Drybath, Thermo Fisher Scientific, Madison, USA) at 95 and 140 rpm, respectively. The total digestion time for gastric and pancreatin juices was one and four hours, and sampling was performed every 10 and 30 min, respectively. The peptide content in the samples was determined by a modified Lowry method (Hartree, 1972), and the rate of diffused peptides was calculated as the ratio of peptides mass that was released during the GI simulation, and the total peptides mass that was inserted on beginning of the process.

## 2.7. Statistical analysis

The statistical analysis of the data was performed using OriginPro 9.0 software (Origin Lab Corporation, MA, SAD). A comparison of the means was ascertained by Tukey's test at 5 % significance level using one-way analysis of variance (ANOVA). All experiments were carried out in triplicate and the experimental results were expressed as mean value  $\pm$  standard deviations (SD).

## 3. Results and discussion

### 3.1. Effect of encapsulation process parameters on the efficiency

The produced Neutrase-Flavourzyme hydrolysate of soy protein was characterized in terms of raw protein content ( $76.68 \pm 2.55$  % per d.m.), amino acid composition (Supplementary material, Table S3), as well as content of free amino acids (Supplementary material, Table S4).

The content of hydrophilic and hydrophobic amino acids was 49.96 g/100 g of proteins and 36.53 g/100 g of proteins, respectively, while only  $0.582 \pm 0.022$  meq Leu/g of proteins and  $1.170 \pm 0.025$  meq Pro/g of proteins were released by the action of used proteases, determined via the ninhydrin protocol. In order to better understand the effect of process parameters on the efficiency of hydrolysate encapsulation, the MW distribution of peptides in the hydrolysate obtained by ultrafiltration was determined as well as free amino acid content. It appeared that the Neutrase-Flavourzyme hydrolysate contained mainly moderate molecular weight peptides of 30 kDa (~30 %) and between 10 and 30 kDa (~45 %), while the content of low MW peptides with 3–10 kDa (~16 %) was lower, and with just a few percentages yield of the free amino acids in the fraction with MW < 1 kDa (~4%).

The encapsulation efficiency appears to be an important process parameter determining the ability of loading the soy protein hydrolysate into liposome carriers. Thus, the influence of phospholipid (0.01–0.10 g/mL) and peptide (50–200 mg/g of phospholipids) concentrations on the encapsulation efficiency was investigated (Fig. 1). Concurrently, the effect of ultrasound treatment during the preparation of liposome carriers was considered in regard to obtain nanocarriers.

It seems clear that by increasing the initial peptide concentrations, the encapsulation efficiency of soy hydrolysates is increased significantly ( $p < 0.05$ ), in the case of both preparation protocols, without and with ultrasound treatment (Fig. 1A). By using lipid concentration of 0.02 g/mL the highest encapsulation efficiency of  $20.09 \pm 0.67$  % has been achieved in the liposomes treated with ultrasound when maximum amount of hydrolysate has been offered (200 mg/g of phospholipids). Varying the phospholipid concentration (Fig. 1B), the efficiency has been shown to increase significantly ( $p < 0.05$ ) up to  $33.41 \pm 1.75$  % achieved with the concentration of 0.03 g/mL, and then a decline was detected. The observed decrease can be attributed to the repulsion between the zwitterionic phosphatidylcholine in the liposomes and the charged side chains of the oligopeptides from soy protein hydrolysate, occurred more intensively at high lipid concentrations. Also, the complex structure of the used Phospholipon®90G affects the electrostatic and hydrophobic interactions between soybean peptides and phospholipids making them different from those of pure phosphatidylcholine (PC). In general, EE depends on many factors: type and purity of the carrier phospholipid material and protein nature play an important role in addition to core-to-wall ratio, the conditions at which encapsulation is carried out, and production method utilized. Literature data show moderate to high EE values for protein hydrolysates. Corrêa et al. (2019) who used the same purified PC as the one used in this study and applied nearly the same production protocol, reported a value of 48 % for sheep

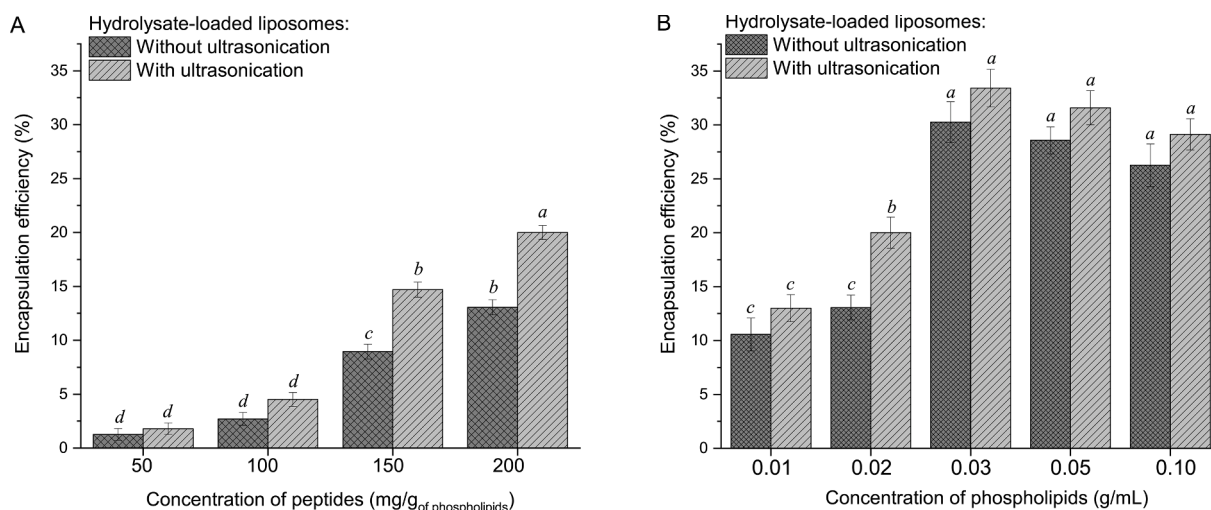
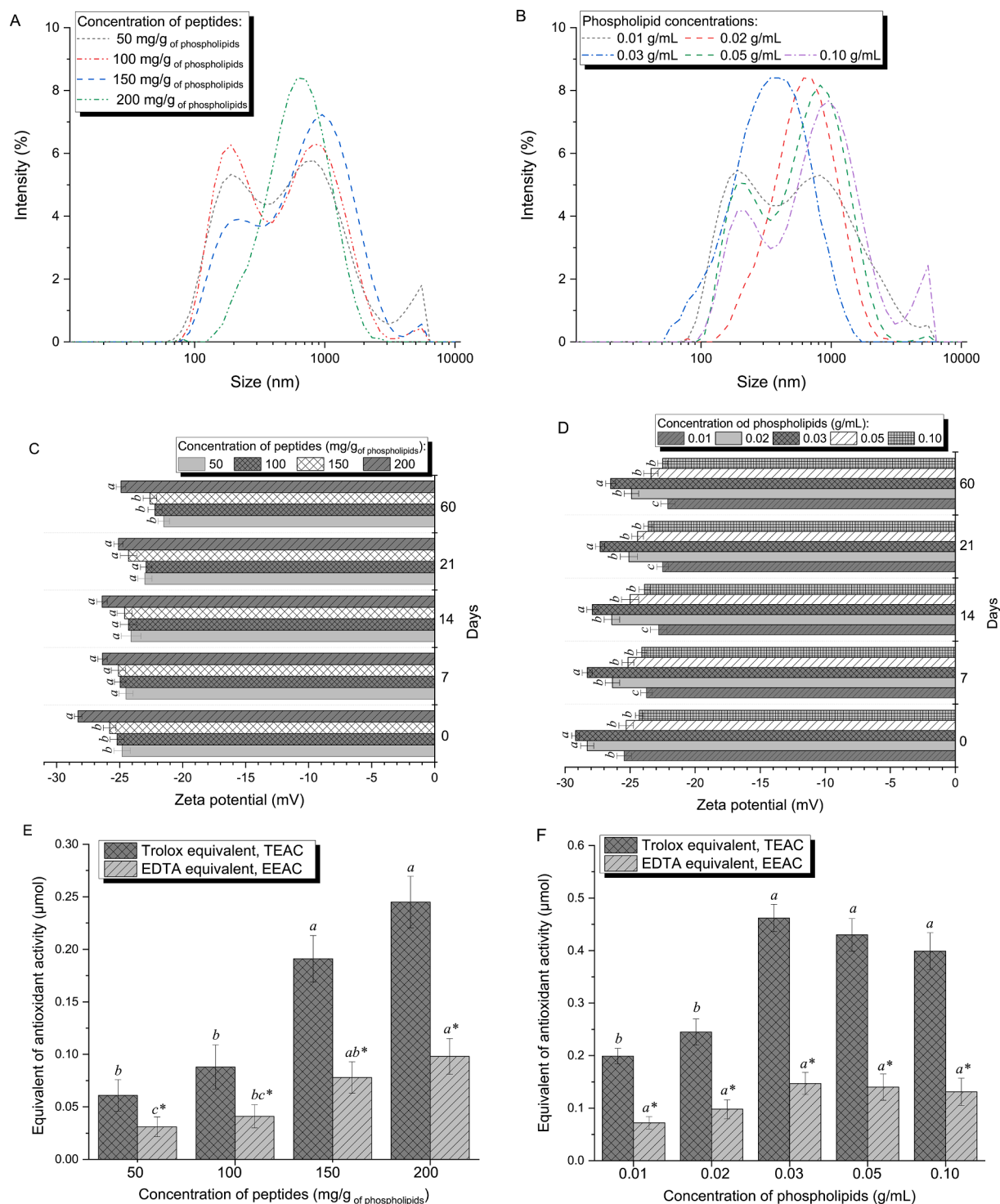


Fig. 1. The influence of peptides (A) and phospholipid (B) concentrations on the encapsulation efficiency of soy protein hydrolysate. The data are presented as the mean  $\pm$  SD ( $n = 3$ ). Means with different letters in the same figure are significantly different ( $p < 0.05$ ).

wehy hydrolysate, but using more than doubled higher protein to lipid ratio (0.263 versus 0.133). Obviously, the electrostatic interactions dependent on phospholipid and protein charge affect liposome capacity to encapsulate.

Overall, it is evident that the sonication showed a positive correlation with the *EE* of soy protein hydrolysate (Fig. 1A and 1B), indicating that no thermal degradation of phospholipids occurred. Thermal degradation was prevented by a constant cooling of the liposome

suspensions during the ultrasound probe treatment. Literature data state that only 1.6 % of the initial amount of PC hydrolyzed at 50 °C during 24 h (Rabinovich-Guilatt et al., 2005), as well as that the generation of free radicals by ultrasound and hereof the oxidation of PC has been absent (Silva, Little, Ferreira, & Cavaco-Paulo, 2008). The achieved *EE* higher by 0.6 to 7 % in ultrasonicated liposome suspensions (Fig. 1A and 1B) can be ascribed to cavitation effect leading the amelioration of electrostatic and hydrophobic interaction between the phospholipids



**Fig. 2.** Particle size distribution (A and B),  $\zeta$  potential (C and D) and antioxidant activity (E and F) of soy hydrolysate-loaded liposomes created with ultrasonication influenced by the peptide and the phospholipid concentrations. The data are presented as the mean  $\pm$  SD ( $n = 3$ ). Means with different letters for the same analyzed day (C and D) are significantly different ( $p < 0.05$ ). Means with different letters in the same figure (E and F) are significantly different ( $p < 0.05$ ).

and soy peptides in hydrolysates. Also, the multilamellar hydrolysate-loaded liposome vesicles created without sonication, appear to become unilamellar under the sonication effect. It is critical to highlight that all experiments, were carried out with phospholipid samples following chloroform evaporation and consecutive drying procedures of the generated thin film, all with the goal of eliminating of unpleasant solvent to the greatest extent. The removal of chloroform in the thin film has been confirmed by FTIR analysis (Supplementary material, Fig. S1), suggesting the safety of the phospholipid film formation according to the derived protocol for further application and analysis, although this does not rule out its existence in ppm, which is otherwise permitted by food or pharmaceutical regulations.

### 3.2. Physicochemical characteristics of hydrolysate-loaded liposome carriers

As previously reported, the SPH enriched in bioactive peptides was successfully encapsulated into liposomes, especially when an ultrasound-assisted hydration technique used. So, in the second part of the research, primarily hydrolysate-loaded liposomes prepared with ultrasound treatment were analyzed. Particle size distribution, average diameter,  $\zeta$  potential and polydispersity light scattering analysis were appraised at the day of encapsulation, and also during liposome storage (Fig. 2, Table S1 and Fig. S1).

Fig. 2.

The average particle size increases with increasing peptide concentrations (Table S1), and herein for the liposomes fabricated with a peptide concentration of 200 mg/g of phospholipids, without and with ultrasound treatment, are graded at 3464 and 342.2 nm, respectively. In general, the ultrasound treatment leads to the depletion of particle size and the formation of unilamellar from multilamellar liposomes. The unimodal particle distribution curve is observed only when peptide concentration of 200 mg/g of phospholipids has been used (Fig. 2A), while with lower amount of peptides the bimodal distribution curves are observed, (Fig. 2A), and confirmed by polydispersity values (Table S1). The larger ultrasonicated hydrolysate-loaded liposomes are also observed to have a lower PDI compared ( $p < 0.05$ ) to non-sonicated liposomes, and it is likely that net hydrolysate charge and interaction with individual amino acid residues affected the liposome dispersion. On the other hand, higher concentration of peptides is predicted to expand the vesicle, as larger number of peptides is entrapped, resulting in the larger mean particle diameter of created liposomes. This has been demonstrated and coincided with literature research (Corrêa et al., 2019; Mohan, Rajendran, Thibodeau, Bazinet, & Udenigwe, 2018; Sarabandi et al., 2019b; Sarabandi, Mahoonak, Hamishehkar, Ghorbani, & Jafari, 2019a). As a rule, augmentation of the phospholipid concentration from 0.01 to 0.1 g/mL means bigger vesicles, thus a rise from 2742 to 3562 nm and from 316.4 to 558.4 nm is seen for non-sonicated and sonicated formulations, respectively (Table S1). It seems obvious that more concentrated suspensions of multilamellar liposomal vesicles offer higher resistance to deformations caused by ultrasound or other physical treatments, as well as higher aggregate partition resistance (Barnadas-Rodríguez, & Sabés, 2001). Analyzing the distribution curve (Fig. 2B), it can be seen that liposomes created with lipid concentration of 0.03 g/mL exhibit the most uniform distribution, as confirmed with the lowest PDI index of 0.315 (Table S1). As for the liposomes produced with other phospholipid concentrations, a multimodal distribution can be observed with the PDI index above 0.300 suggesting heterogenous vesicle populations.

Hydrolysate-loaded liposomes have a negative value of  $\zeta$  potential (-24 to -34 mV), that represent indicator of their physical stability in aqueous suspensions (Fig. 2C and D). The obtained charge strongly affects liposomal solutions stability, since at higher values of this potential, the stronger electrostatic repulsions occur between the liposome carriers in aqueous solution, preventing aggregation. The negative value of  $\zeta$  potential increases in the range from -25 to -29 mV with the

peptide concentration increase from 50 to 200 mg/g of phospholipids, suggesting that surface hydrophobicity and the electrical charge of the amino acid residues of encapsulated peptides have important contribution in net charge. Furthermore, these values remain negative throughout the two-month period (60 days), with no significant decrease during this period. It is interesting to point out that absolute  $\zeta$  potential values of the ultrasound-assisted liposomes (Fig. 2B and C) are significantly lower ( $p < 0.05$ ) compared to the non-sonicated liposomes (Fig. S2). The above is a consequence of structural reorganization of the multilamellar liposomal membrane, as well as of the hydrolysate peptide structural changes involving reorientation of amino acid residues. Minutely, liposome vesicles created with initial peptide concentration of 200 mg/g of phospholipids have  $\zeta$  potential of -32.9 and -28.3 mV, while the measured values with initial phospholipid concentration of 0.03 g/mL are -30.1 and -29.2 mV for non-sonicated and sonicated liposome suspensions, respectively. Regardless of the liposome preparation method, all prepared liposome suspensions show good storage stability for 60 days at 4 °C, most likely as a consequence of hydrophobic interactions between the phospholipids and peptides.

Recently, soy protein concentrate and isolate hydrolysates have been receiving increasing attention owing to their antioxidant activity (Chatterjee, Gleddie, & Xiao, 2018; Jovanović et al., 2019; Chen et al., 2020; Chen et al., 2021). Herein, taking into consideration the encapsulation efficiency, average particle size, size distribution and stability, we have determined the ABTS<sup>•+</sup> radical scavenging and ferrous ion chelating activities of ultrasound-assisted hydrolysate-loaded liposomes (Fig. 2E and F). As can be seen from the experimental results, the activities of antioxidant equivalents are significantly increased ( $p < 0.05$ ) in hydrolysate-loaded liposomes, which is attributed to the capacity of the peptides for radical scavenging and chelation. Antioxidant activities of encapsulated peptides are in accordance with the encapsulation efficiency; the low antioxidant activity is observed when the encapsulation efficiency (Fig. 1) is also lower, and *vice versa*. It is evident that the initial increase of peptide concentration leads to the statistically significant ( $p < 0.05$ ) augmentation of ABTS<sup>•+</sup> radical scavenging and Fe<sup>2+</sup> chelating activities, and the highest activities of  $0.245 \pm 0.025$   $\mu\text{mol TE}$  (i.e.,  $17.94 \pm 0.89$  %) and  $0.098 \pm 0.017$   $\mu\text{mol EE}$  ( $14.40 \pm 0.78$  %), respectively, are noticed with an initial concentration of 200 mg/g of phospholipids. The significant enhancement of antioxidant activities ( $p < 0.05$ ) has been realized by increasing phospholipid concentration up to 0.03 g/mL, after which significant changes are not noticeable ( $p$  greater than 0.05). The greatest values are  $0.462 \pm 0.026$   $\mu\text{mol TE}$  (i.e.,  $33.80 \pm 0.90$  %) and  $0.147 \pm 0.021$   $\mu\text{mol EE}$  (i.e.  $21.70 \pm 0.79$  %). This is evidence that the encapsulation process has not impaired the biological activity of the peptides in soy hydrolysate. Encapsulated peptides still exhibit a great ability to donate protein or electrons an unstable ABTS<sup>•+</sup> radical cation, as well as to form a chelate complex with unstable ferrous ions. It can be emphasized that an increase in the free hydrophobic amino acids or hydrophilic antioxidant amino acids would increase the free radical inhibitors of ABTS (Corrêa et al., 2019; Ramezanzade, Hosseini, Akbari-Adergani, & Yaghmur, 2021; Sarabandi, Mahoonak, Hamishehkar, Ghorbani, & Jafari, 2019a). As proof of the above, peptide samples which concentration corresponded to the concentration of the encapsulated peptides were subjected to an antioxidant assay (Table S2). Comparing the results of both free soy hydrolysate and encapsulated soy hydrolysate, it can be concluded that the addition of Phospholipon®90G contributes partly to the total antioxidant activity, only 3 to 4 % and 4 to 5 %, for different concentration of peptide and phospholipid, respectively. This contribution is attributed to the composition of Phospholipon®90G that contains a small amount of well-known antioxidants, vitamin E – tocopherol, and is coincided with the empty liposome samples (controls; about 4 and 5 % of scavenge and chelation, respectively). The reason can be attributed to the inefficiency of Phospholipon®90G structure in inhibiting the water-soluble ABTS<sup>•+</sup> radical, and in chelating ferrous ions. Sarabandi et al. (2019a) investigated the antioxidant activity of nanoliposomes loaded with hydrolysate



or peptides from enzymatic hydrolysis of casein, and also confirmed that the encapsulation process did not impair the activity of the peptide. As we previously reported, the antioxidant activity of the used soy protein hydrolysates was positively related to the high content of hydrophobic amino acids (Pavlović et al., 2020), and was consistent with the results of Chen et al. (2020) who shown that the antioxidant behavior of soy protein isolate hydrolysates was influenced by its amino acid composition.

### 3.3. Effect of cholesterol addition on the physical characteristics of hydrolysate-loaded liposome

Finally, the influence of the addition of lipid membrane stabilizers has been considered. Recently, the use of cholesterol as a stabilizer was conducted and it appeared that this steroid can: 1) increase the packing of phospholipid molecules; 2) decrease the bilayer permeability to non-electrolyte and electrolyte solutes; 3) ameliorate the resistance to aggregation; and 4) prolong the release of the active substance at the target site of action (Briuglia et al., 2015; Pinilla et al., 2020). So, by adopting the ultrasound-assisted hydration protocol of the thin film created with the most desirable phospholipid concentration (0.03 g/mL), the various concentrations of peptides combined with cholesterol addition were examined in order to increase the amount of trapped peptides and the stability of liposome suspensions. The obtained results regarding physicochemical characteristics are presented in the Table 1, while the results of controlled release and lipid peroxidation studies are given in the Fig. 3.

It seems that the cholesterol addition greatly increases the encapsulation efficiency (Table 1), and even approximately twice the efficiency is achieved with the peptides of 200 mg/g of phospholipids compared with the liposome without cholesterol (approx. 60 %;  $p < 0.05$ ). This indicates that, due to the high hydrophobicity, cholesterol has been shown to be very effective in strengthening the packaging of phospholipid bilayers. Hereof, it reduces membrane permeability, which certainly contributes to a higher encapsulation efficiency (Briuglia et al., 2015; Pinilla et al., 2020). According to the stabilization of lipid vesicles in the presence of cholesterol, and a high encapsulation efficiency of soy protein hydrolysates, the low mean particle size has been detected, from 191.1 to 286.7 nm, and measured PDI value ranges from 0.254 to 0.392. For the sake of comparison, liposomes created by peptide concentration of 200 mg/g of phospholipids and cholesterol have a mean particle size of 193.5 nm, while the size of its cholesterol-free counterpart is 356.2 nm. The introduction of cholesterol into the liposomal system also shows a more stable trend and a more uniform distribution of particle size (Fig. 3A). It is assumed that the enhanced effect of ultrasound treatment and low cholesterol concentration contributed to a decrease in the mean diameter of liposome carriers. Furthermore, it is noticed that the addition of cholesterol contributed to the higher absolute values of  $\zeta$  potential improving the stability of the hydrolysate-loaded liposome carriers, and an increase in the absolute value of the  $\zeta$  potential with an increase in peptide concentration is observed. The best value of  $\zeta$  potential seems to be  $-34.6$  mV. So, it can be inferred that the cholesterol presence in the bilayer leads to decrease in the affinity of the surface

cation binding, which induces an increase in the negative value of  $\zeta$  potential.

Parallel to the improved stability and encapsulation, as well as depletion of average carrier size, the preservation of peptide antioxidant activities has been recorded (Table 1). The degree of ABTS<sup>•+</sup> scavenging and Fe<sup>2+</sup> chelation values increased markedly ( $p < 0.05$ ) in hydrolysate-loaded liposomes, being attributed to the radical scavenging capacity of the latter (from 50 to 200 mg/g of phospholipids). The maximal values of  $0.654 \pm 0.029$   $\mu\text{mol TE}$  (i.e.,  $47.90 \pm 1.45$  %) and  $0.220 \pm 0.047$   $\mu\text{mol EE}$  (i.e.,  $32.35 \pm 1.53$  %) are achieved. In this case, too, it has been confirmed that antioxidant activity, whether radical scavenging or ferrous chelating, originates from exclusively encapsulated peptides, and that the phospholipid and cholesterol contribution is minimal (empty liposome vesicles possess only approx. 3.6 % of radical scavenging and chelating activities).

After a more detailed analysis of the influence of various process parameters mentioned above, the ultrasound-assisted hydrolysate-loaded liposomes fabricated by phospholipids at 0.03 g/mL, peptides at 200 mg/g of phospholipids originated from hydrolysate, and cholesterol (0.33 % w/v) were subjected to analysis of lipid peroxidation. The lipid peroxidation inhibition activity was analyzed by *in vitro* test in a model system with linoleic acid, and was studied during 7 days. The obtained results are given in Fig. 3B. It is evident that the inhibitory effect of linoleic acid oxidation is obtained for samples containing soy peptides, namely soy hydrolysate (non-encapsulated; SPH) and liposomes containing encapsulated soy protein hydrolysate (SHLc). During the first day of incubation, mild increase of the absorbance can be noticed for soy hydrolysate and hydrolysate-loaded liposomes. Taking into account the whole incubation time (from 2 to 6 days), this increase is not significant. On the other hand, the mean values of the degree of linoleic acid oxidation of  $15.12 \pm 1.25$  and  $11.02 \pm 1.41$  % are determined, in the presence of soy hydrolysate (SPH) and hydrolysate-loaded liposome (SHLc), respectively. These results are very satisfactory, and confirm the ability of created soy peptides to participate in oxidative stress and/or lipid peroxidation chain reactions, donating protons and/or electrons, to unstable intermediates. The highest inhibition ability has vitamin C – ascorbic acid, which is the positive control,  $7.75 \pm 1.03$  %. Comparing the ability of ascorbic acid and soy peptides to inhibit the oxidation of linoleic acid, soy peptides can be considered very successful protectors, because only 4 % more linoleic acid reacted in their presence. In both cases, the amount of reacted linoleic acid increases slightly after 4 days, although it is considerably lower ( $p < 0.05$ ) in the presence of hydrolysate-loaded liposomes than in free hydrolysate. Besides, the empty liposomes show no ability to inhibit the oxidation of linoleic acid, thus confirming that in the case of hydrolysate-loaded liposomes, the high inhibition ability originates only from the peptides themselves, and also that in some ways, the liposome membrane acts protectively on encapsulated peptides and allows its gradual release and reaction with intermediates. The degree of linoleic acid oxidation in the presence of empty liposomes is amounted at  $62.42 \pm 1.23$  %. Earlier literature studies have confirmed that soy protein hydrolysates possess effective lipid peroxidation inhibition ability (Chen et al., 2020; Chen et al., 2021), while Peña-Ramos, & Xiong (2003) have emphasized that soy

**Table 1**

Encapsulation efficiency, average size, polydispersity index (PDI),  $\zeta$  potential, and antioxidant activity of liposomes with cholesterol.

Soy hydrolysate-loaded liposomes created with cholesterol						
$m_{\text{peptides}}$ (mg)	EE* (%)	Average size (nm)**	PDI	$\zeta$ potential (mV)	Trolox equivalent, TEAC ( $\mu\text{mol}$ )	EDTA equivalent, EEAC ( $\mu\text{mol}$ )
12.5	$43.3 \pm 1.85^b$	$286.7 \pm 15.96^a$	$0.392 \pm 0.002^a$	$-25.5 \pm 0.785^b$	$0.478 \pm 0.036^c$	$0.177 \pm 0.018^b$
25.0	$47.5 \pm 1.68^b$	$225.2 \pm 20.36^b$	$0.308 \pm 0.015^b$	$-31.3 \pm 0.693^a$	$0.519 \pm 0.015^b$	$0.192 \pm 0.023^a$
37.5	$56.3 \pm 2.65^a$	$191.1 \pm 14.79^b$	$0.266 \pm 0.036^c$	$-33.1 \pm 0.823^a$	$0.612 \pm 0.048^a$	$0.223 \pm 0.038^a$
50.0	$60.5 \pm 2.16^a$	$193.5 \pm 28.93^b$	$0.254 \pm 0.018^c$	$-34.6 \pm 0.984^a$	$0.654 \pm 0.029^a$	$0.220 \pm 0.047^a$

\* EE means encapsulation efficiency.

\*\* Empty liposome without and with cholesterol have particle size 180.5 and 183.6 nm respectively.

Results are expressed as mean  $\pm$  standard deviation ( $n = 3$ ). Means with different letters in the same column are significantly different ( $p < 0.05$ ).



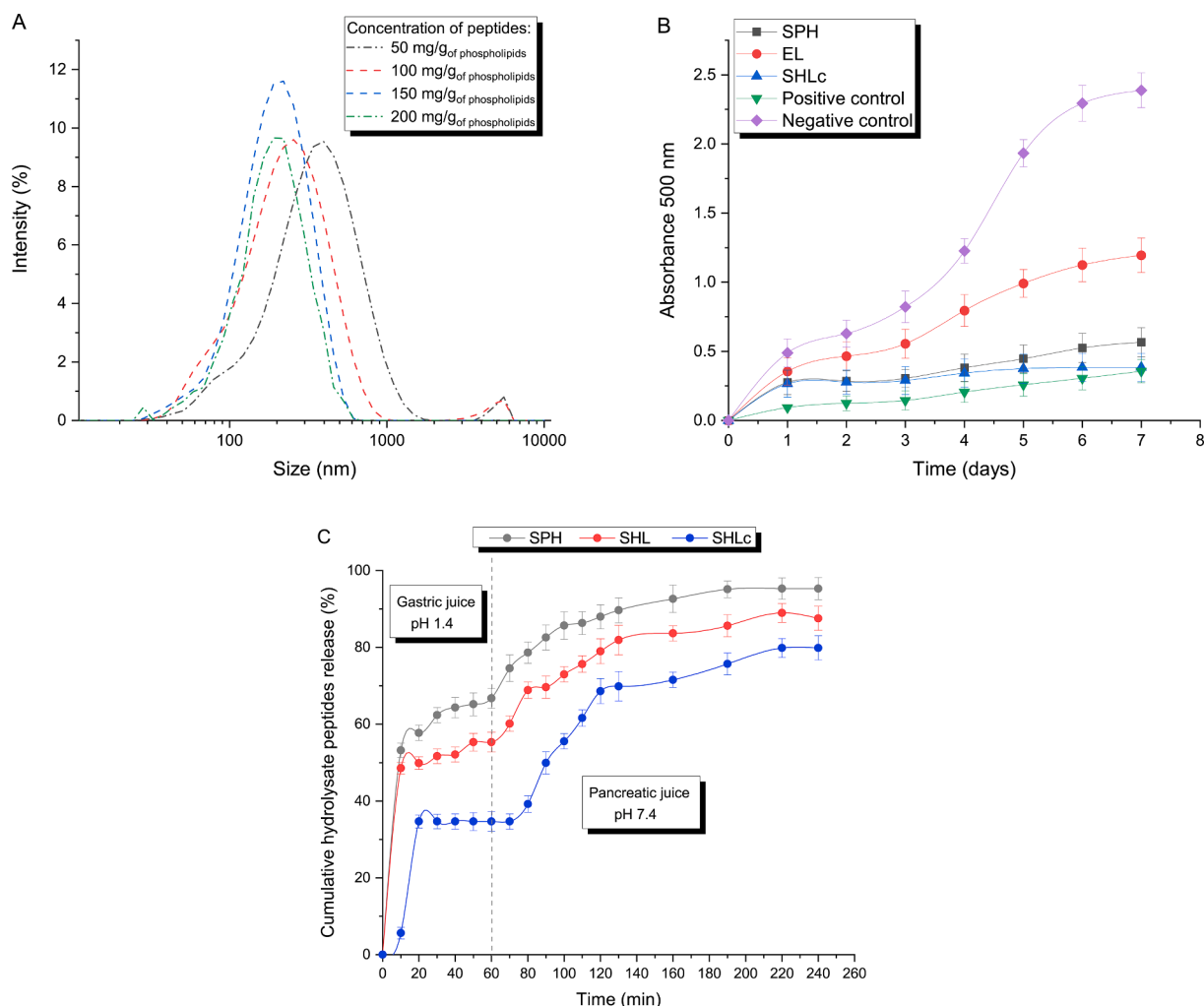


**Fig. 3.** Particle size distribution (A), lipid peroxidation inhibition activity (B) and *in vitro* gastrointestinal digestion (C) of soy hydrolysate-loaded liposomes fabricated with stabilizer cholesterol. The data are presented as the mean  $\pm$  SD ( $n = 3$ ). *Legends: SPH is soy protein concentrate hydrolysate, SHL is soy hydrolysate-loaded liposome, SHLc is soy hydrolysate-loaded liposome with cholesterol addition, EL is empty liposome.*

hydrolysates were significantly more efficient at lipid inhibition compared with other protein hydrolysates. In general, the presented results indicate that the soy proteins hydrolysate has antioxidant activity that remains preserved after their encapsulation in liposomes, and which is a consequence of the amino acid composition of the peptide in the hydrolysate. Moreover, the amino acid residues' hydrophobicity in the hydrolysate can hasten the peptide-linoleic acid interactions, which has a protective effect, meaning it inhibits the oxidation of linoleic acid.

Finally, the fabricated liposomes were characterized regarding the controlled release of encapsulated peptides. For this purpose, *in vitro* digestion catalyzed by pepsin and pancreatin was carried out in a batch system in which hydrolysate-loaded liposomes were immersed in gastric and pancreatic juice, respectively, to simulate GI circumstances. The peptide release from the liposomes was measured at various time intervals, and the findings are presented in Fig. 3C.

It is obvious that digestion by pepsin and pancreatin lead to the release of soy peptides from liposome carriers. After one hour of digestion by pepsin, the percentage of diffused peptides from the hydrolysate-loaded liposome (SHL) is amounted at  $55.32 \pm 2.56$  %, while the percentage of non-encapsulated hydrolysate (SPH) is  $66.72 \pm 2.59$  %. The release of peptides from the hydrolysate-loaded liposome created with cholesterol (SHLc) is amounted at  $34.67 \pm 2.57$  %, indicating slower kinetics of the peptide release induced by cholesterol presence. Digestion with pancreatic juice has been monitored for the next 4 h, and the

percentage of diffused peptides from SHLc has been the lowest ( $79.85 \pm 3.14$  %). Significantly higher ( $p < 0.05$ ) cumulative peptides release of  $87.55 \pm 3.04$  and  $95.32 \pm 2.89$  % is measured from SHL and SPH, respectively. Thus, the instability of non-encapsulated hydrolysate was demonstrated, indicating that liposomes had a better stability into simulated GI conditions. Precisely, the stability of liposomes in the gastric environment was significantly higher ( $p < 0.05$ ) compared to the stability in the intestinal environment. According to literature, low pH does not affect the stability and basic characteristics of liposomes, and in simulated gastric conditions, the percentage of peptides loss is low,  $\sim 20$  % (Liu et al., 2012). Our results are in contrast with these results, which imply that low pH and pepsin digestion have an impact on created liposome structure causing peptide release. Moreover, a  $\sim 50$  % of diffused soy peptides at the end of pancreatin digestion can be attributed to the hydrolysis of phosphatidylcholine by pancreatin, and interaction of bile salts with liposome components. Pancreatin contains lipolytic enzymes such as lipase, phospholipase and cholesterol esterase, responsible for phospholipid lipolysis and the formation of various products such as lysophospholipids that do not have a two-layer structure and make unstable micelles, which at the end leads to increased permeability of lipid membranes. This is in agreement with the literature data (Liu et al., 2012).

### 3.4. Structural and morphological characteristics of soy hydrolysate-loaded liposome

Structural characteristics of fabricated liposomes have been performed in order to assess the presence of interaction between phospholipids and soy hydrolysate. The structural changes of the samples have been monitored in the range 4000–500  $\text{cm}^{-1}$  (Fig. 4) by FTIR analysis.

A change in the structure of the protein hydrolysate can be seen at 1400  $\text{cm}^{-1}$ , which is a characteristic of C–N stretching vibration, as well as a minor change at 1340  $\text{cm}^{-1}$  assigned to C–O stretching vibrations of amide III. Changes in the range 1500–1650  $\text{cm}^{-1}$  are related with the amid I (C–O stretching vibrations) and amide II (N–H deformations and stretching C–H vibrations). Comparing spectra of the empty liposomes (EL) and hydrolysate-loaded liposomes (SHLc), differences in the range of 2850 to 2950  $\text{cm}^{-1}$  can be noticed, characteristic for asymmetric C–H<sub>2</sub> stretching vibrations. The mentioned vibrations indicate the presence of a flexible acyl chain in the lipid membrane (Bilge et al., 2014). There is a small shift in the same range, from 2924 to 2922  $\text{cm}^{-1}$  after the encapsulation, as a result of the ionic interactions between the phospholipids and the peptides. The peak at 1735  $\text{cm}^{-1}$  of the empty liposome (EL), coming from the stretching C=O vibrations of the aliphatic stearic acid chain and the functional group is shifted to 1738  $\text{cm}^{-1}$  after the encapsulation, suggesting the existence of hydrogen bonds between carbonyl (C=O) groups of the phospholipid and the hydrolysate (Bilge, Sahin, Kazanci, & Severcan, 2014; Sarabandi, Mahoonak, Hamishehkar, Ghorbani, & Jafari, 2019a). The present band in the range 1040–1230  $\text{cm}^{-1}$  is characteristic for the stretching PO<sub>2</sub> vibrations (Bilge et al., 2014). Higher/lower frequencies in this range indicate the presence/absence of hydrogen bonds between phosphate groups and the hydrogen atom of bioactive molecules. In the liposomes with encapsulated hydrolysate, the shift is towards lower frequencies, from 1052 to 1048  $\text{cm}^{-1}$ . The same behavior is noticed after encapsulation of the casein hydrolysates (Sarabandi et al., 2019a). The band at 978  $\text{cm}^{-1}$  from the blank liposome can be ascribed to the asymmetric stretching vibrations of choline (N-(CH<sub>3</sub>)<sub>3</sub>) in the phospholipid's polar region. Overall, the FTIR spectra confirm the existence of the interaction between the phospholipid's functional groups and the peptides side chains from the soy protein hydrolysate.

Scanning electron microscopy (SEM) and transmission electron microscopy (TEM) imaging are widely used to study the morphological and size properties of nanoparticles. SEM and TEM studies revealed the

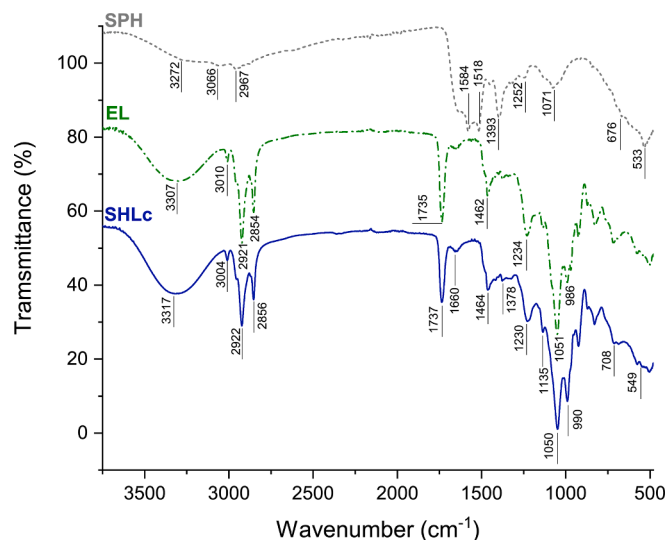


Fig. 4. FTIR spectra of hydrolysate-loaded liposomes created with ultrasound-assisted protocol. Legends: SPH is soy protein concentrate hydrolysate, SHLc is soy hydrolysate-loaded liposome with cholesterol addition, EL is empty liposome.

development of almost spherical nanovesicles with smooth exterior surfaces (Fig. 5). Many features of lipid nanocarriers, including physical and chemical durability, encapsulation efficiency, loading capacity, location of bioactive chemicals within the nanoparticles, and compound release rate, have been shown to be highly impacted by nanoparticle shape (Sarabandi et al., 2019a). The given images of scanning electron microscope (SEM) from the structural and surface properties of empty (EL), hydrolysate-loaded liposome (SHL) and hydrolysate-loaded nanoliposome stabilized with cholesterol (Fig. 5A, B and C, respectively) indicate that there is no difference in surface properties of the nanoparticles. However, the two important characteristics are noticeable and concern the increase of liposome sizes after encapsulation of soy hydrolysate and denser clusters of spherical nanoparticles with smooth surfaces. Sarabandi et al., 2019a loaded flaxseed protein hydrolysates within nanoliposomes, and investigated the effect of freeze-drying process of nanoliposomes on the morphology of particles. The results revealed the laminar and broken structures with lots of surface pores as result of freeze-drying process, but the spherical and shrunk carriers with a reservoir-type structure were dominant.

TEM images indicate and confirm the individual unilamellar vesicles with spherical morphology of fabricated nanoliposomes. It can be noticed that empty liposome (Fig. 5D) appears without a distinct core, while the hydrolysate-loaded nanoliposomes have the clearly defined cores, with a shell around it, assumably a lipid layer. In both, DLS and TEM measurements, the measured particle sizes of empty liposomes coincided (183.6 nm). Hydrolysate-loaded nanoliposomes retain the spherical shape of the core after encapsulation. The unilamellar vesicles (Fig. 5E) have been created by loading hydrolysate within liposomes without cholesterol (SHL), and the measured average size of particles are coincided (356.2 and 353.8 nm, respectively DLS and TEM). It is worth noting that the particle size of SHLc nanoliposomes detected by TEM (Fig. 5F) is much larger (237.0 nm) than the mean values obtained by DLS (193.5 nm). These two findings indicate the formation of tiny unilamellar vesicles (SUV). The above discrepancies in measuring principles between the two methodologies might explain this disparity; DLS measurements are considered in terms of light intensity and the hydrodynamic diameter of the particle, whereas TEM data are measured directly. It is worth noting that similar TEM images have been previously reported on phosphatidylcholine and lecithin-based liposomes with encapsulated peptides and/or protein hydrolysates (Ramezanzade et al., 2021; Sepúlveda et al., 2021).

## 4. Conclusions

In this study, the antioxidant peptides originated from the soy protein concentrate hydrolysate were loaded into the nanoliposome carriers by the thin film method. Ultrasound-assisted technique, during the hydration stage of encapsulation process, provided small unilamellar vesicles by reducing the size of peptide-loaded liposomes 9.5 times in average and increased encapsulation efficiency (EE) from 2 to 13 % to 4–20 % depending on the peptide concentrations. Nevertheless, the optimal phospholipids and peptides concentration of 0.03 g/mL and 200 mg/g of phospholipids, respectively, prompted to the higher EE value of 33 %. Physical stability during storage at 4 °C for 2 months was confirmed by steady negative  $\zeta$  potential values of all tested liposome formulations. The cholesterol addition at concentration of 0.33 % (w/v) intensively increased EE to 60.5 %, diminished vesicle size to 193.5 nm, increased stability (-35 mV) and reduced cumulative peptide release to 80 % upon 4 h of *in vitro* gastrointestinal digestion. Antioxidant activity of encapsulated soy peptides expressed via radical scavenging and chelating abilities, and lipid peroxidation inhibitory activity remained unchanged after the ultrasound-assisted encapsulation process. Finally, the fabricated novel nanoliposomes with encapsulated antioxidant peptides from soy hydrolysate can be considered as a potential functional food supplement.

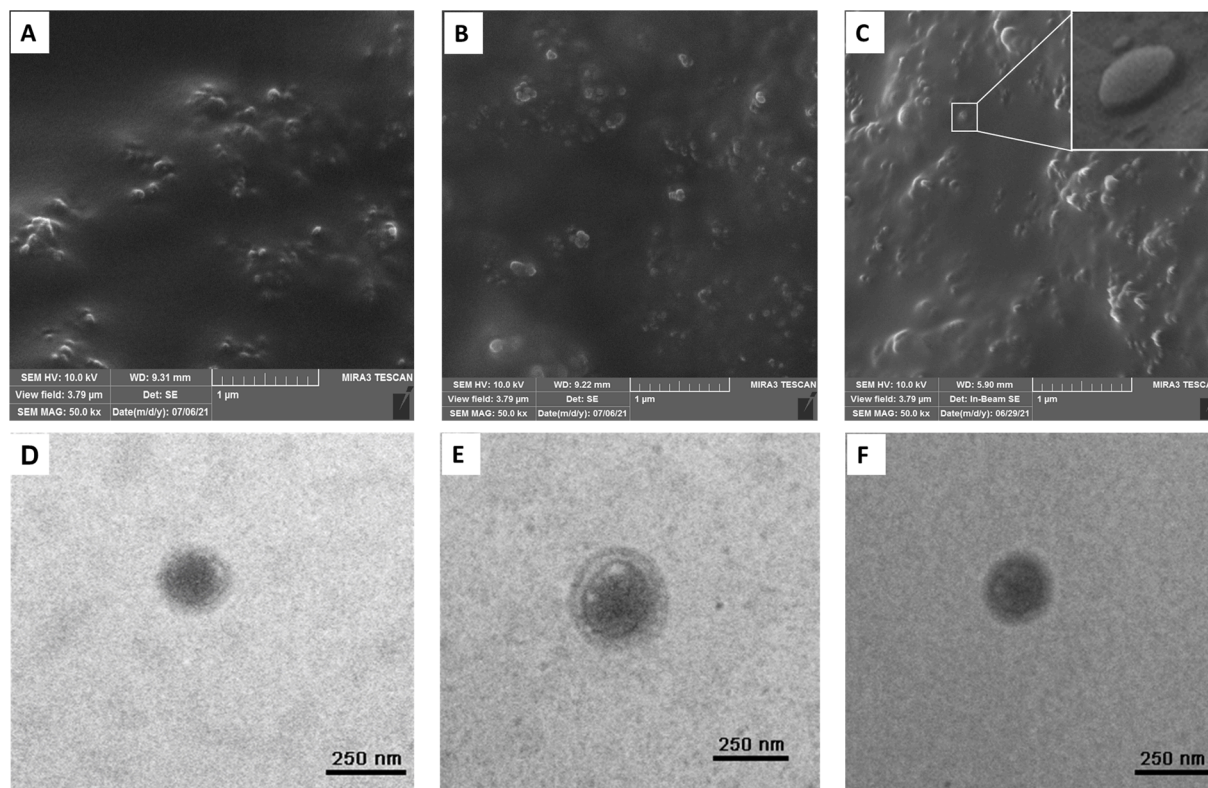


**Fig. 5.** Scanning (A, B and C; magnification 50000x) and transmission (D, E and F; magnification 17000x) electron micrograph of empty liposome vesicles (EL), ultrasound-assisted hydrolysate-loaded liposomes (SHL), and ultrasound-stabilized hydrolysate-loaded liposomes stabilized with cholesterol (SHLC). (Reaction conditions: negative staining of liposomes with uranyl acetate (3%; pH 3) were performed for monitoring TEM morphology).

### Declaration of Competing Interest

The authors declare that they have no known competing financial interests or personal relationships that could have appeared to influence the work reported in this paper.

### Acknowledgments

The authors are grateful for the financial support from the Ministry of Education, Science and Technological Development of the Republic of Serbia (Contract No. 451-03-68/2022-14/200287 and Contract No. 451-03-68/2022-14/200135).

### Author contributions

Conceptualization: Z.K.-J., V.Đ. and J.M.; Methodology: N.P., Z.K.-J. and D.P.; Software: N.P. and D.P.; Validation: J.M. and V.Đ.; Formal analysis: N.P., J.M. and V. Đ.; Investigation: N.P. and J.M.; Resources: Z. K.-J. and B.B; Data curation: N.P. and J.M.; Writing – original draft: N.P. and J.M.; Writing – review & editing: V.Đ. and Z.K.-J.; Visualization: J. M., N.P., and D.P.; Supervision: Z.K.-J. and B.B; Project administration: Z.K.-J. and B.B; Funding acquisition: Z.K.-J. and B.B.

### Appendix A. Supplementary data

Supplementary data to this article can be found online at <https://doi.org/10.1016/j.fochx.2022.100370>.

### References

Barnadas-Rodríguez, R., & Sabés, M. (2001). Factors involved in the production of liposomes with a high-pressure homogenizer. *International Journal of Pharmaceutics*, 213(1), 175–186. [https://doi.org/10.1016/S0378-5173\(00\)00661-X](https://doi.org/10.1016/S0378-5173(00)00661-X)

- Bilge, D., Sahin, I., Kazanci, N., & Severcan, F. (2014). Interactions of tamoxifen with distearoyl phosphatidylcholine multilamellar vesicles: FTIR and DSC studies. *Spectrochimica Acta Part A: Molecular and Biomolecular Spectroscopy*, 130, 250–256. <https://doi.org/10.1016/j.saa.2014.04.027>
- Briuglia, M.-L., Rotella, C., McFarlane, A., & Lamprou, D. A. (2015). Influence of cholesterol on liposome stability and on in vitro drug release. *Drug Delivery and Translational Research*, 5(3), 231–242. <https://doi.org/10.1007/s13346-015-0220-8>
- Chang, C. Y., Jin, J. D., Chang, H. L., Huang, K. C., Chiang, Y. F., Ali, M., & Hsia, S. M. (2021). Antioxidative Activity of Soy, Wheat and Pea Protein Isolates Characterized by Multi-Enzyme Hydrolysis. *Nanomaterials (Basel, Switzerland)*, 11(6), 1509. <https://doi.org/10.3390/nano11061509>
- Chatterjee, C., Gleddie, S., & Xiao, C.-W. (2018). Soybean bioactive peptides and their functional properties. *Nutrients*, 10(9), 1211. <https://doi.org/10.3390/nu10091211>
- Chen, C., Sun-Waterhouse, D., Zhang, Y., Zhao, M., & Sun, W. (2020). The chemistry behind the antioxidant actions of soy protein isolate hydrolysates in a liposomal system: Their performance in aqueous solutions and liposomes. *Food Chemistry*, 323, Article 126789. <https://doi.org/10.1016/j.foodchem.2020.126789>
- Chen, C., Sun-Waterhouse, D., Zhao, J., Zhao, M., Waterhouse, G. I. N., & Sun, W. (2021). Soybean protein isolate hydrolysates-liposomes interactions under oxidation: Mechanistic insights into system stability. *Food Hydrocolloids*, 112, Article 106336. <https://doi.org/10.1016/j.foodhyd.2020.106336>
- Corrêa, A. P. F., Bertolini, D., Lopes, N. A., Veras, F. F., Gregory, G., & Brandelli, A. (2019). Characterization of nanoliposomes containing bioactive peptides obtained from sheep whey hydrolysates. *LWT - Food Science and Technology*, 101, 107–112. <https://doi.org/10.1016/j.lwt.2018.11.036>
- Culetu, A., Duta, D. E., Knežević-Jugović, Z., Jovanović, J., Šekuljica, N. & Stefanović, A. (2018, October). Influence of soy protein hydrolysates on the rheological characteristics of wheat dough. Conference paper presented at the 4<sup>th</sup> International Congress “Food Technology, quality and safety” (FoodTech), Novi Sad, Serbia, Book of Abstracts, page 18, ISBN 978-86-7994-054-4.
- Culetu, A., Duta, D. E., Knežević-Jugović, Z., Jovanović, J., Šekuljica, N., Comaniciu, D. L., & Ordodi, L. V. (2019, September). Soy protein hydrolysates in bakery products. Conference paper presented at the 4<sup>th</sup> International Conference on Metrology in Food and Nutrition (IMEKOFOODS), Brussels – Tervuren, Belgium, Book of Abstracts, [https://www.imeko.org/publications/tc23-2019/imekofoods4\\_book\\_of\\_abstracts\\_september\\_2019.pdf](https://www.imeko.org/publications/tc23-2019/imekofoods4_book_of_abstracts_september_2019.pdf).
- Daroit, D. J., & Brandelli, A. (2021). In vivo bioactivities of food protein-derived peptides – a current review. *Current Opinion in Food Science*, 39, 120–129. <https://doi.org/10.1016/j.cofs.2021.01.002>
- Gomaa, A. I., Martinent, C., Hammami, R., Fliss, I., & Subirade, M. (2017). Dual coating of liposomes as encapsulating matrix of antimicrobial peptides: Development and characterization. *Frontiers in Chemistry*, 5(NOV). <https://doi.org/10.3389/fchem.2017.00103>. Article 103.



- Görgüç, A., Gençdağ, E., & Yılmaz, F. M. (2020). Bioactive peptides derived from plant origin by-products: Biological activities and techno-functional utilizations in food developments – A review. *Food Research International*, 136, Article 109504. <https://doi.org/10.1016/j.foodres.2020.109504>
- Hartree, E. F. (1972). Determination of protein: A modification of the lowry method that gives a linear photometric response. *Analytical Biochemistry*, 48(2), 422–427. [https://doi.org/10.1016/0003-2697\(72\)90094-2](https://doi.org/10.1016/0003-2697(72)90094-2)
- Kjeldahl Method (ISO 5983-1:2005). *Animal Feeding Stuffs: Determination of Nitrogen Content and Calculation of Crude Protein Content. Part 1: Kjeldahl Method*; International Organization for Standardization: Geneva, Switzerland, 2005.
- Jash, A., Ubeyitogullari, A., & Rizvi, S. S. H. (2021). Liposomes for oral delivery of protein and peptide-based therapeutics: Challenges, formulation strategies, and advances. *Journal of Materials Chemistry B*, 9(24), 4773–4792. <https://doi.org/10.1039/d1tb00126d>
- Jovanović, J., Stefanović, A., Culetu, A., Duta, D., Luković, N., Tanasković, S. J., ... Knežević-Jugović, Z. (2019). Enzymatic treatment of soy protein concentrate: Influence on the potential techno-functional and antioxidant properties. *Journal of Hygienic Engineering and Design*, 30, 58–68. <https://www.scopus.com/inward/record.uri?eid=2-s2.0-85083296266&partnerID=40&md5=6e427517480a5e6b68eb67b4250ce1ec>
- Knežević-Jugović, Z., Culetu, A., Duta, D., Mohan, G., Jovanović, J., Stefanović, A., Sekuljica, N., & Dordević, V. (2018, May). *Enzymatic hydrolysis as a tool for enhancing antioxidant capacity and sensory qualities of soy proteins*. Conference paper presented at the meeting of 9<sup>th</sup> Central European Congress on Food (CEFood), Sibiu, Romania. Book of Abstract, page 110, ISBN 978-606-12-1546-1.
- Krobthong, S., Yingchutrakul, Y., Visessanguan, W., Mahatnirunkul, T., Samutrtai, P., Chaichana, C., Papan, P., & Choowongkamon, K. (2021). Study of the lipolysis effect of nanoliposome-encapsulated *Ganoderma lucidum* protein hydrolysates on adipocyte cells using proteomics approach. *Foods*, 10(9). <https://doi.org/10.3390/foods10092157>. Article 2157.
- Li, T., Zhang, X., Ren, Y., Zeng, Y., Huang, Q., & Wang, C. (2022). Antihypertensive effect of soybean bioactive peptides: A review. *Current Opinion in Pharmacology*, 62, 74–81. <https://doi.org/10.1016/j.coph.2021.11.005>
- Li, Z., Paulson, A. T., & Gill, T. A. (2015). Encapsulation of bioactive salmon protein hydrolysates with chitosan-coated liposomes. *Journal of Functional Foods*, 19, 733–743. <https://doi.org/10.1016/j.jff.2015.09.058>
- Liu, W., Ye, A., Liu, C., Liu, W., & Singh, H. (2012). Structure and integrity of liposomes prepared from milk- or soybean-derived phospholipids during in vitro digestion. *Food Research International*, 48(2), 499–506. <https://doi.org/10.1016/j.foodres.2012.04.017>
- Luo, P., & He, D. P. (2018). Preparation of liposome encapsulating angiotensin-I-converting enzyme inhibitory peptides from sunflower protein hydrolysates. *Molecular Medicine Reports*, 17(4), 5306–5311. <https://doi.org/10.3892/mmr.2018.8474>
- Mazloomi, S. N., Mahoonak, A. S., Ghorbani, M., & Houshmand, G. (2020). Physicochemical properties of chitosan-coated nanoliposome loaded with orange seed protein hydrolysate. *Journal of Food Engineering*, 280, Article 109976. <https://doi.org/10.1016/j.jfoodeng.2020.109976>
- McClements, D. J. (2014). *Nanoparticle- and microparticle-based delivery systems: Encapsulation, protection and release of active compounds* (1st ed.). CRC Press, 10.1201/b17280.
- Memarpoor-Yazdi, M., Asoodeh, A., & Chamani, J. (2012). A novel antioxidant and antimicrobial peptide from hen egg white lysozyme hydrolysates. *Journal of Functional Foods*, 4(1), 278–286. <https://doi.org/10.1016/j.jff.2011.12.004>
- Mohammadi, M., Hamishehkar, H., Ghorbani, M., Shahvalizadeh, R., Pateiro, M., & Lorenzo, J. M. (2021). Engineering of liposome structure to enhance physicochemical properties of Spirulina plantensis protein hydrolysate: Stability during spray-drying. *Antioxidants*, 10(12). <https://doi.org/10.3390/antiox10121953>
- Mohan, A., Rajendran, S. R. C. K., He, Q. S., Bazinet, L., & Udenigwe, C. C. (2015). Encapsulation of food protein hydrolysates and peptides: A review. *RSC Advances*, 5(97), 79270–79278. <https://doi.org/10.1039/c5ra13419f>
- Mohan, A., Rajendran, S. R. C. K., Thibodeau, J., Bazinet, L., & Udenigwe, C. C. (2018). Liposome encapsulation of anionic and cationic whey peptides: Influence of peptide net charge on properties of the nanovesicles. *LWT - Food Science and Technology*, 87, 40–46. <https://doi.org/10.1016/j.lwt.2017.08.072>
- Nkanga, C. I., Bapoliisi, A. M., Okafor, N. I., & Krause, R. W. M. (2019). General perception of liposomes: formation, manufacturing and applications. In A. Catala (Ed.), *Liposomes - advances and perspectives* (pp. 4–11). IntechOpen. <https://dx.doi.org/10.5772/intechopen.84255>.
- Pavlović, N. V., Jovanović, J. R., Dordević, V. B., Bugarski, B. M., & Knežević-Jugović, Z. D. (2020). Production and characterization of liposomes with encapsulated bioactive soy protein hydrolysate. *Hemijska industrija*, 74(5), 327–339. <https://doi.org/10.2298/hemind200530030p>
- Peña-Ramos, E. A., & Xiong, Y. L. (2003). Whey and soy protein hydrolysates inhibit lipid oxidation in cooked pork patties. *Meat Science*, 64(3), 259–263. [https://doi.org/10.1016/S0309-1740\(02\)00187-0](https://doi.org/10.1016/S0309-1740(02)00187-0)
- Pinilla, C. M. B., Reque, P. M., & Brandelli, A. (2020). Effect of oleic acid, cholesterol, and octadecylamine on membrane stability of freeze-dried liposomes encapsulating natural antimicrobials. *Food and Bioprocess Technology*, 13(4), 599–610. <https://doi.org/10.1007/s11947-020-02419-8>
- Rabinovich-Guillat, L., Dubernet, C., Gaudin, K., Lambert, G., Couvreur, P., & Chaminade, P. (2005). Phospholipid hydrolysis in a pharmaceutical emulsion assessed by physicochemical parameters and a new analytical method. *European Journal of Pharmaceutics and Biopharmaceutics*, 61(1), 69–76. <https://doi.org/10.1016/j.ejpb.2005.03.001>
- Ramezanzade, L., Hosseini, S. F., Akbari-Adergani, B., & Yaghmur, A. (2021). Cross-linked chitosan-coated liposomes for encapsulation of fish-derived peptide. *LWT - Food Science and Technology*, 150, Article 112057. <https://doi.org/10.1016/j.lwt.2021.112057>
- Sarabandi, K., Jafari, S. M., Mohammadi, M., Akbarbaglu, Z., Peshzki, A., & Khakbaz Heshmati, M. (2019b). Production of reconstitutable nanoliposomes loaded with flaxseed protein hydrolysates: Stability and characterization. *Food Hydrocolloids*, 96, 442–450. <https://doi.org/10.1016/j.foodhyd.2019.05.047>
- Sarabandi, K., Mahoonak, A. S., Hamishehkar, H., Ghorbani, M., & Jafari, S. M. (2019a). Protection of casein hydrolysates within nanoliposomes: Antioxidant and stability characterization. *Journal of Food Engineering*, 251, 19–28. <https://doi.org/10.1016/j.jfoodeng.2019.02.004>
- Sepúlveda, C. T., Alemán, A., Zapata, J. E., Montero, M. P., & Gómez-Guillén, M. C. (2021). Characterization and storage stability of spray dried soy-rapeseed lecithin/trehalose liposomes loaded with a tilapia viscera hydrolysate. *Innovative Food Science & Emerging Technologies*, 71, Article 102708. <https://doi.org/10.1016/j.ifset.2021.102708>
- Silva, R., Little, C., Ferreira, H., & Cavaco-Paulo, A. (2008). Incorporation of peptides in phospholipid aggregates using ultrasound. *Ultrasonics Sonochemistry*, 15(6), 1026–1032. <https://doi.org/10.1016/j.ultsonch.2008.03.010>
- Starcher, B. (2001). A ninhydrin-based assay to quantitate the total protein content of tissue samples. *Analytical Biochemistry*, 292(1), 125–129. <https://doi.org/10.1006/abio.2001.5050>
- Tkaczewska, J. (2020). Peptides and protein hydrolysates as food preservatives and bioactive components of edible films and coatings - A review. *Trends in Food Science and Technology*, 106, 298–311. <https://doi.org/10.1016/j.tifs.2020.10.022>
- Xu, J., Jiang, S., Liu, L., Zhao, Y., & Zeng, M. (2021). Encapsulation of oyster protein hydrolysates in nanoliposomes: Vesicle characteristics, storage stability, in vitro release, and gastrointestinal digestion. *Journal of Food Science*, 86(3), 960–968. <https://doi.org/10.1111/1750-3841.15606>
- Zhao, C. J., Schieber, A., & Gänzle, M. G. (2016). Formation of taste-active amino acids, amino acid derivatives and peptides in food fermentations – A review. *Food Research International*, 89(1), 39–47. <https://doi.org/10.1016/j.foodres.2016.08.042>